New Fluorimetric Alkali and Alkaline Earth Metal Cation Sensors Based on Noncyclic Crown Ethers by Means of Intramolecular Excimer Formation of Pyrene

Yoshio Suzuki, Tatsuya Morozumi, and Hiroshi Nakamura*

Division of Material Science, Graduate School of Environmental Earth Science, Hokkaido University, Sapporo 060-0810, Japan

Masatsugu Shimomura

Molecular Device Laboratory, Research Institute for Electronic Science, Hokkaido University, Sapporo 060-0812, Japan

Takashi Hayashita

Department of Chemistry, Graduate School of Science, Tohoku University, Aoba-ku Sendai 980-77, Japan

Richard A. Bartsh

Department of Chemistry and Biochemistry, Texas Tech University, Lubbock, Texas 79409

Received: March 19, 1998; In Final Form: July 28, 1998

New fluorescent reagents, 2,2′-[oxybis(3-oxapentamethyleneoxy)]-bis[*N*-(1-pyrenylmethyl)benzamide)] (**4**) and its analogues (**2**, **3**, and **5**) which have two pyrenes at the both terminals of polyoxyethylene compounds, were synthesized, and their complexation behavior with alkaline earth cations was investigated by fluorescence spectrometry, fluorescence lifetimes, and ^{1}H NMR spectrometry. These reagents (**3**−**5**) showed strong intramolecular excimer emissions around at 480 nm in the fluorescence spectra. On the complexation with alkaline earth metal cations, the increase of monomer emission around at 400 nm accompanied by the disappearance of intramolecular excimer emission of free reagents was observed. These reagents formed a 1:1 complex, and the order of complex formation constants was $Ca^{2+} \cong Sr^{2+} > Ba^{2+} > Mg^{2+} > Li^+$ for all reagents. ^{1}H NMR spectra of these complexes with alkaline earth cations suggested the helical structures of the complexes. Fluorescence spectral changes at the formation of complexes depended on the chain length of the oxyethylene moiety and metal cations. In all cases, the formation of helical structures at the complexation was supported by the ^{1}H NMR spectra.

Introduction

It is known that tetraethylene glycol dimethyl ether (glyme), poly(ethylene glycol), and their ethers solvate salts of alkali metals.[1,2] Although these noncyclic ether derivatives do not show a strong complexation ability compared to that of crown ethers,[3] the conformation of these compound changes drastically from a linear structure to a pseudocyclic one upon the complex formation with metal ions. Thus, noncyclic crown ether derivatives have received much attention, and various attempts have been reported to improve their low binding ability for metal ions, e.g., the formation of the pseudocyclic structure through head-to-tail interaction on noncyclic crown ethers. The pseudocyclic structure increases the binding force and plays important roles not only in artificial ionophores but also in natural ionophores for the selective binding of metal cations. Monensin is a naturally occurring noncyclic ion carrier which is constructed with three tetrahydrofuran units and two pyran units having hydroxyl and carboxyl groups at their terminals.[4,5] In alkaline conditions monensin forms the pseudocyclic structure like a crown ether molecule via intramolecular head-to-tail hydrogen bonds between the carboxylate anion and hydroxyl group.

An early study on artificial noncyclic crown ether derivatives, called podand, was carried out by Vögtle et al.[6,7] They demonstrated that oligo-oxyethylene compounds appending quinoline units at their terminals bind K^+ strongly via electrostatic interaction between the ion and oxygen atoms with the aid of $\pi-\pi$ interaction between end-capped quinolines. Their study also showed that quinoline moieties, which can be strong ligands themselves, provide an increase in rigidity around the oxyethylene part and significantly contribute to stabilization of the complex with K^+. Thus, artificial noncyclic polyether compounds have been used for an ion selective ionophore as active cation transport and extraction reagents.

Nakahama et al.[8−11] demonstrated that a series of synthetic carboxylic ionophores exhibit high selectivity for K^+ over Na^+ in the ion transport experiment across the dichloromethane liquid membrane. This excellent selectivity for K^+ was explained by the high lipophilicity of helical K^+ complex. This idea was further supported by X-ray crystal structure analysis.[12,13] Some podand derivatives incorporating ionophoric functional groups such as carboxylic acid, hydroxyl group,[14] and quinoline[15,16] located at the terminals of molecules exhibit an excellent property as metal ion carriers. These ionophores revealed a reversible conformational change between the pseudocyclic and linear structures using interactions between hydroxyl group or quinoline moiety and carboxylate anion. Recently, a noncyclic polyether dicarboxylic acid ionophore was employed as an

S1089-5647(98)01567-3 CCC: $15.00

extraction reagent for the separation of Pb^{2+} from weakly acidic aqueous solutions by liquid chloroform membranes.[17]

If the conformational change of a noncyclic crown ether is converted into physical signals, such as UV absorption and fluorescence, etc., one can develop metal ion sensors more sensitive than crown ethers. On the basis of this idea, we recently synthesized novel fluorescent reagents that have two fluorescent chromophores (anthracene, pyrene, fluorene, etc.) symmetrically or asymmetrically placed at both terminals of 1,13-diamino-4,7,10-trioxatridecane, and their complexations with alkali and alkaline earth cations were examined.[18,19] The complexations brought a shift of the emission maximum shifted from 400 to 490 nm. This indicated that the two anthracenes adopted in stack conformation upon ion complexation. A fluorescent regent containing two asymmetric fluorescent chromophores (one side was anthracene (electron donor) and the other was anthraquinone (electron acceptor)) gave quenching of the emission of the anthracene monomer upon the addition of alkaline earth cations. Anthracene approaches anthraquinone upon complexation, and a rapid electron-transfer quenching of the anthracene excited state occurs. In these cases, the order of complex formation constants of both complexes was $Ca^{2+} > Sr^{2+} > Ba^{2+} > Mg^{2+}$. A large fluorescence maximum shift and the quenching of anthracene fluorescence are a clear indication of the binding event.

Moreover, one can expect that if the chain length at the oxyethylene moiety becomes long, a structural change upon the formation of a complex will be significantly increased. The large conformational change is favorable for making ion and molecular sensing systems.[20−24] However, the lower complex formation constants and selectivity against metal cations will decrease with increased chain length. Thus, we considered two points in synthesizing a new fluorimetric noncyclic crown ether: (a) formation of pseudocyclic structure as a binding site and (b) increase of rigidity at the oxyethylene part.

(a) As is well-known, two pyrene molecules tend to stack and form an excimer.[25,26] This strong interaction enabled us to monitor dynamics of cyclizations of polymer chains by means of fluorescence spectroscopies by using α,ω-dipyrenyl reagents as probes: poly(styrene),[27] poly(ethylene oxide),[28] poly(tetramethylene oxide),[29] poly(dimethylsiloxane),[30] poly(bisphenol A-diethylene glycol carbonate),[31] and 1,8-bis[[(1-pyrenylmethoxy)-carbonyl]ethyl]perfluorooctane.[32] A similar method was used to determine the effect of dissociated carboxylic acid groups on hydrogen bonding with poly(methacrylic acid).[33] Besides, a detection system of guest molecules and ions was also reported by use of fluorescence changes[20] in intramolecular excimer emission and fluorescence quenching of pyrene functionalized calix[4]arene,[34−36] homotrioxacalix[3]arene,[37] calix[4]-resorcinarene,[38] and cyclodextrin.[39] These observation prompted us to introduce pyrene at the end of polyether as a reporting moiety and attachment for constructing the pseudocyclic structure.

(b) The increase of rigidity at the oxyethylene part will be expected to increasing binding constants. We thus planned to introduce two benzenes at both terminals where carbonyl oxygen atoms were located at the ortho position of the benzene ring. This molecular design may produce high complex formation constants through strong coordination of carbonyl oxygen atoms to metal cations.

On the basis of the above, we synthesized a new type of fluorescent reagents **2**−**5**, bearing two pyrenes connected via an amide linkage at the ortho position of the benzene ring at the end of the polyether. Their complexation with alkali and alkaline earth cations was investigated with the use of fluorescence spectrometry, fluorescence lifetimes, and ^1H NMR spectrometry.

SCHEME 1

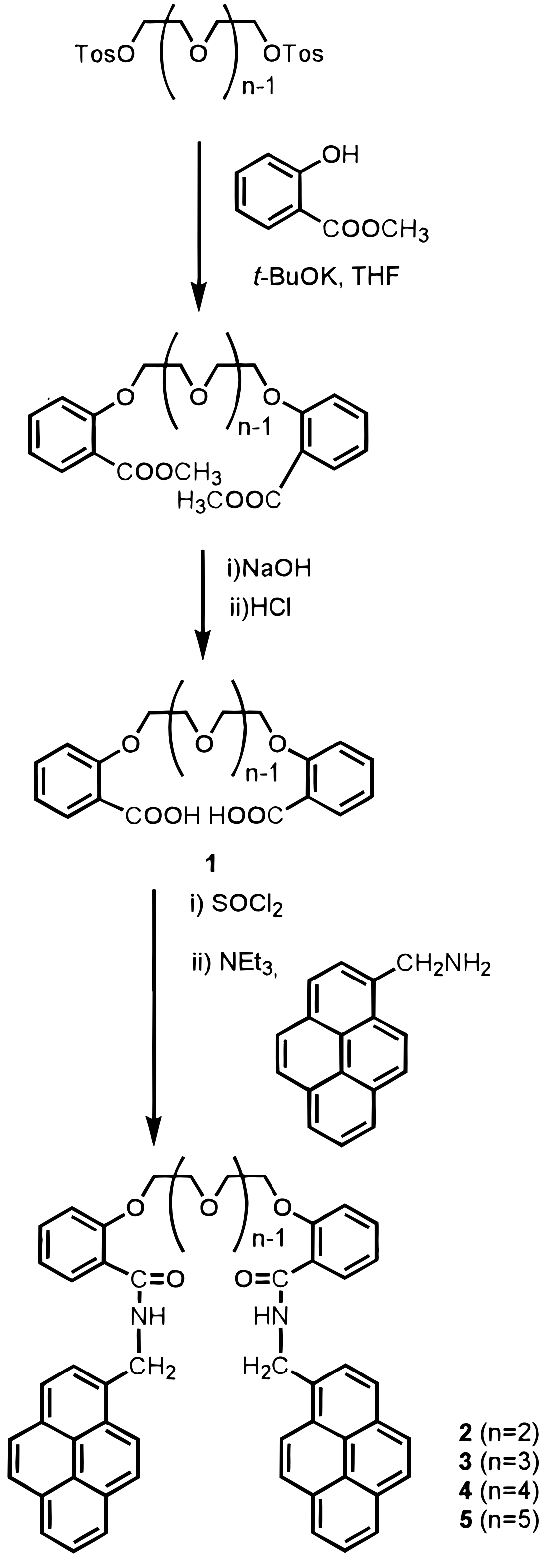

Experimental Section

The synthetic pathway of the compounds **2**−**5** was summarized in Scheme 1. The preparation of polyether−dicarboxylic acids (**1**) was carried out according to the method reported previously.[40]

General Procedure of Syntheses of 2−5. Forty milliliters of $SOCl_2$ was added to the dicarboxylic acid (1.2 mmol) and refluxed for 3 h. Excess $SOCl_2$ was distilled off in vacuo and evaporated after the addition of 10 mL of benzene four times, and the corresponding acid chloride was obtained. 1-Pyrenemethylamine (2.4 mmol) dissolved in 20 mL of chloroform and 1 mL of triethylamine were added dropwise to this acid chloride in an ice bath. The mixture was stirred for 1 day, washed with 30 mL of water three times, and dried over $MgSO_4$. The solvent was evaporated in reduced pressure, and the residue was purified by silica gel column chromatography (eluent: chloroform−ethyl acetate). These compounds were confirmed by ^{1}H NMR spectra and elemental analyses.

*2,2′-[Oxybis(ethyleneoxy)]-bis[N-(1-pyrenylmethyl)benzamide] (**2**):* Yield 28.6%. ^{1}H NMR ($CDCl_3$) $\delta = 1.76$ (C−CH_2−O, t, 4H), 2.20 (−C−CH_2−O, t, 4H), 5.16 (Ar−CH_2, d, 2H), 5.49 (aromatic, d, 2H), 6.97 (aromatic, t, 2H), 7.07 (aromatic, t, 2H), 7.85 (aromatic, d, 2H), 7.90 (NH, t, 2H), 7.95−8.23 (aromatic, m, 20H). Found: C, 79.41; H, 5.33; N, 3.56%. Calcd for $C_{52}H_{40}O_5N_2{\cdot}{}^1/_2H_2O$: C,78.90; H, 5.31; N, 3.54%.

*2,2′-[(Ethylenedioxy-bis(ethyleneoxy)]-bis[N-(1-pyrenylmethyl)benzamide] (**3**)*: Yield 30.5%. ^{1}H NMR (acetonitrile-d_3) $\delta = 2.20$ (C−CH_2−O, s, 4H), 2.91 (−C−CH_2−O, t, 4H), 3.63 (−C−CH_2−O, t, 4H), 5.11 (Ar−CH_2, d, 2H), 6.72 (aromatic, d, 2H), 7.02 (aromatic, t, 2H), 7.34 (aromatic, t, 2H), 8.01 (aromatic, d, 2H), 7.90−8.25 (aromatic, m, 20H), 8.34 (NH, m, 2H). Found: C, 78.56; H, 5.65; N, 3.28%. Calcd for $C_{54}H_{44}O_6N_2{\cdot}{}^1/_2H_2O$: C, 78.45; H, 5.45; N, 3.38%.

*2,2′-[Oxybis(3-oxapentamethyleneoxy)]-bis[N-(1-pyrenylmethyl)benzamide] (**4**)*: Yield 25.5%. ^{1}H NMR (acetonitrile-d_3) $\delta = 2.42$ (−C−CH_2−O, t, 4H), 2.60 (−C−CH_2−O, t, 4H), 3.19 (−C−CH_2−O, t, 4H), 3.86 (−C−CH_2−O, t, 4H), 5.18 (Ar−CH_2, d, 2H), 6.84 (aromatic, d, 2H), 7.05 (aromatic, t, 2H), 7.38 (aromatic, t, 2H), 8.08 (aromatic, d, 2H), 7.85−8.25 (aromatic, m, 20H), 8.48 (NH, m, 2H). Found: C, 77.53; H, 5.90; N, 3.24%. Calcd for $C_{56}H_{48}O_7N_2{\cdot}{}^1/_2H_2O$: C, 77.32; H, 5.63; N, 3.22%.

*2,2′-[Ethylenedioxy-bis(3-oxapentamethyleneoxy)]-bis[N-(1-pyrenylmethyl)benzamide] (**5**)*: Yield 20.5%. ^{1}H NMR (acetonitrile-d_3) $\delta = 2.79$ (−C−CH_2−O, s, 4H), 2.68 (−C−CH_2−O, t, 4H), 2.79 (−C−CH_2−O, t, 4H), 2.79 (−C−CH_2−O, t, 4H), 3.96 (−C−CH_2−O, t, 4H), 5.23 (Ar−CH_2, d, 2H), 6.92 (aromatic, d, 2H), 7.04 (aromatic, t, 2H), 7.37 (aromatic, t, 2H), 7.93−8.35 (aromatic, m, 20H), 8.54 (NH, m. 2H). Found: C, 75.34; H, 6.15; N, 2.71%. Calcd for $C_{58}H_{52}O_8N_2{\cdot}{}^1/_2H_2O$: C, 75.40; H, 5.85; N, 3.03%.

Measurement of Fluorescence Spectra. Fluorescence spectra were measured by a Shimadzu RF-5300PC at 25 °C. Concentrations of fluorescent reagents were 1×10^{-6} mol/dm^3 in purified acetonitrile. Alkaline earth metal cations were added into the solution of fluorescent reagent as perchlorate salts. To prevent nonlinearity of the fluorescence intensities, the excitation wavelength was set to 341 nm, which was an isosbestic point in the absorption spectra. The temperature was maintained at 25 °C.

Measurement of Fluorescence Lifetime. Fluorescence lifetimes were measured by a Horiba NAES-500 at room temperature. Concentrations of fluorescent reagents were 1×10^{-6} mol/dm^3, and those of metal cations were 1×10^{-3} mol/dm^3. The excited wavelength was 350 nm, and the monitored wavelength was 400 and 480 nm. The sample solutions were degassed by the freeze−pump−thaw method. All the experiments were carried out at room temperature.

Measurement of ^{1}H NMR. ^{1}H NMR spectra were measured by a JEOL JNM-EX400 at 30 °C. Concentrations of these reagents were 1×10^{-2} mol/dm^3 in acetonitrile-d_3. In the case of measurements of metal complexes, an excess amount of metal cations was added to these solutions.

Results and Discussion

Parts a and b of Figure 1 show the fluorescence spectra of **4** as functions of concentrations of Li^+ and Ca^{2+} perchlorate in acetonitrile at 25 °C, respectively. Free **4** gave the strong intramolecular excimer emission around at 480 nm and a weak monomer emission around at 400 nm. Fluorescence spectra of **4** (Figure 1a) changed a little even if excess Li^+ was added. In contrast, **4**·Ca^{2+} (Figure 1b) showed a large decrease of the intramolecular excimer emission accompanied by a corresponding increase of the monomer emission. This result suggested that the shape of the molecule in a pyrene moiety varied from the intramolecular excimer conformation to a monomer conformation via binding of Ca^{2+} to oxyethylene moiety and carbonyl oxygen atoms. The fluorescence spectra of **3** only changed by the addition of Li^+ (Figure 1c,d). This result also supported that the same structural change occurred in complex **3**·Li^+ due to the complementarity of the pseudocavity of **3** and ionic diameter of Li^+.

The spectral changes of fluorescence and binding constants for various cations are summarized in Table 1. Compounds **2**−**5** showed no fluorescence spectral changes, and only their excimer emissions were observed in the presence of an excess amount of alkali metal ions (except for Li^+). New fluorescent ionophores (**2**−**5**) of Table 1 will be classified into three groups: the first one (compound **2)** features no spectral change in the presence of any metal ions. The second one (compound **3**) features the fluorescence spectral changes in the presence of only Li^+ and Mg^{2+}. The last one (compounds **4** and **5**) features spectral changes in the presence of all alkaline earth metal ions (except for Mg^{2+}). In the case of group 1, its chain length of oxyethylene is too short to surround metal cations. Thus, the complexation ability was too weak to form any complexes with cations. Compound **3** (group 2) in its free state forms an intramolecular pseudocyclic structure which was supported by the excimer fluorescence emission. Conformational changes will be expected to occur since the oxyethylene part can orient to the ions more suitably because of its cavity size matching the ionic radius of Li^+ or Mg^{2+}. The cavity size of **3** is too small for other alkaline earth metal ions (Ca^{2+}, Sr^{2+}, and Ba^{2+}) to form complexes. Compounds **4** and **5** (group 3) have larger cavities than that of **3** and responded to alkaline earth cations (Ca^{2+}, Sr^{2+}, and Ba^{2+}) whose ionic radii are larger than those of Li^+ and Mg^{2+}.

The successive increase of monomer emission with addition of metal ion will finally cause a complete disappearance of the intramolecular excimer. The fluorescence intensity of the excimer emission of **4** at 480 nm was plotted against the ratio of [metal]/[ligand] (Figure 2). The curve obtained clearly shows the formation of a 1:1 complex with Ca^{2+}. The complex formation constant (K) was evaluated from the curve by means of a nonlinear least-squares curve fitting method (Marquardt's method).[41] Formation constants for other ligands and various cations were also determined in the same way and summarized in Table 1. All the ligands formed 1:1 complexes and preferred alkaline earth cations to alkali cations. Compound **3** shows Li^+ and Mg^{2+} specificity, which may stem from good complementarity between its cavity size and their ionic sizes. On the other hand, compound **4** has about 10 times larger complex formation

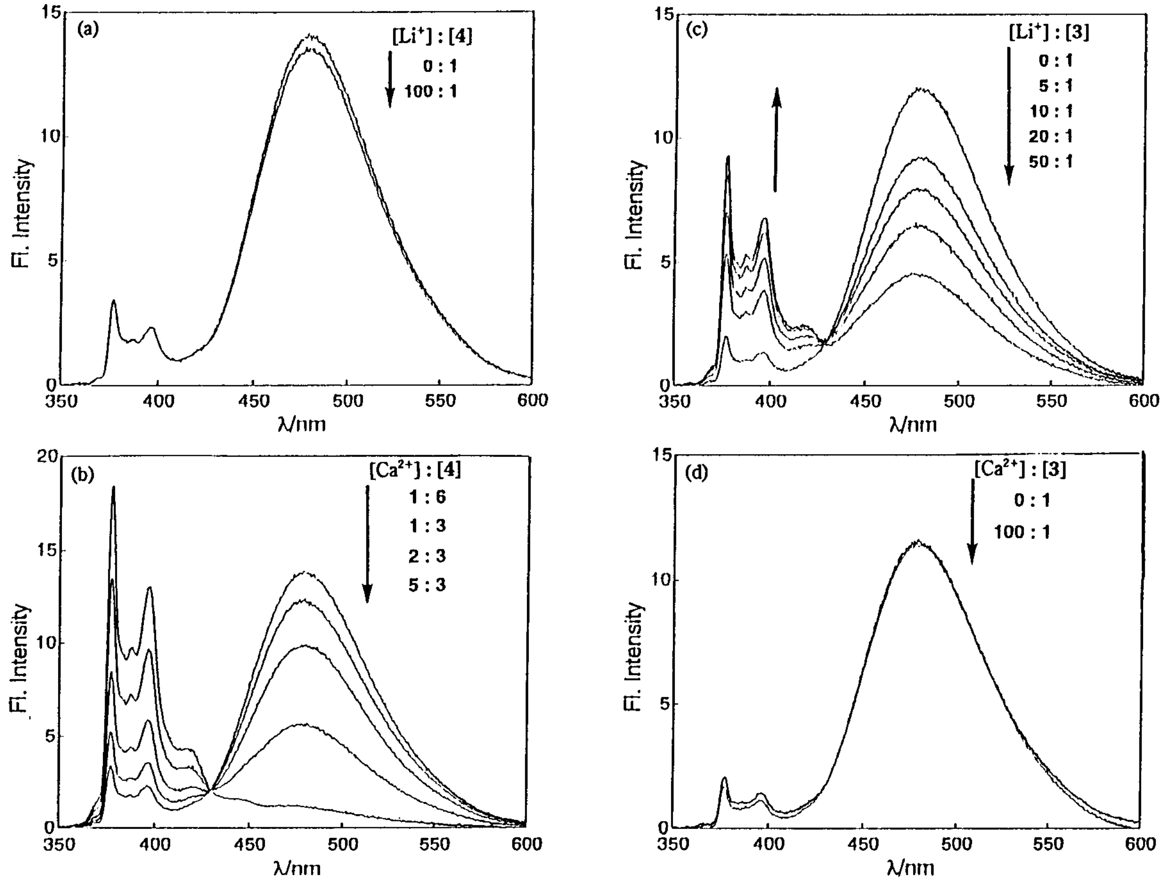

Figure 1. Fluorescence spectra of 4 and its Li^+ complex (a) and Ca^{2+} complex (b); 3 and its Li^+ complex (c) and Ca^{2+} complex (d) in acetonitrile at 25 °C. Excitation wavelength = 341 nm. [3 or 4] = 1×10^{-6} mol/dm^3.

TABLE 1: Summary of Fluorescence Spectral Changes and Complex Formation Constants (log *K*) of 2−5 for Various Metal Ions in Acetonitrile at 25 °C

	Li^+	Na^+	Mg^{2+}	Ca^{2+}	Sr^{2+}	Ba^{2+}
2	*a*	*a*	*a*	*a*	*a*	*a*
3	3.49	*a*	4.61	*a*	*a*	*a*
4	*a*	*a*	5.07	6.57	6.71	5.57
5	*a*	*a*	3.64	6.94	6.33	5.98

[a] These log *K* were not able to be determined because changes of fluorescence spectra were not observed.

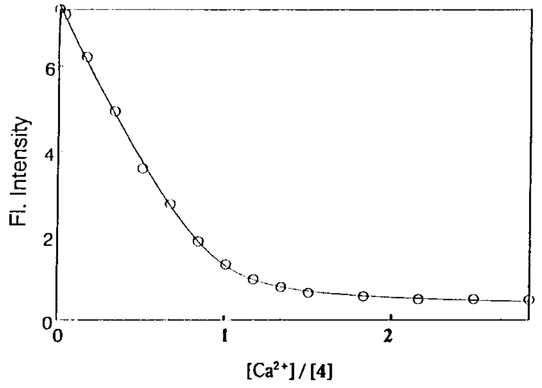

Figure 2. Dependence of fluorescence intensity at 480 nm of **4** on the concentration of Ca^{2+}. Excitation wavelength = 341 nm. [**4**] = 1 $\times 10^{-6}$ mol/dm^3.

constants than those of *N*,*N′*-(4,7,10-trioxatridecane-1,13-diyl)-bis(anthracene-9-carbonamide) with alkaline earth cations as compared with our previous data.[18] This was attributed to the increase of the rigidity of oxyethylene moiety due to the introduction of benzene rings. Presumably, the pseudocyclic structure also contributed to the increase of binding constants.

Fluorescence spectral data clearly indicate structural change of ligands upon complex formation. To clarify the structures of complexes in detail, a ^{1}H NMR study was carried out in the absence and presence of metal cations in acetonitrile-d_3 at 30 °C. The ^{1}H NMR spectra of **4** before and after addition of Ca^{2+} are shown in Figure 3 as a typical result. Peak assignments were made by using H−H COSY and NOESY spectra. The center methylene protons (b and c) of free **4** (and also **3**) exhibited unusually high (ca. 2.2 ppm) upfield chemical shifts. The usual peak position of these oxyethylene protons is ca. 3.5 ppm, and this diamagnetic shift should be due to the aromatic ring current, although the structure was unknown. In the **4**·Ca^{2+} complex, oxyethylene proton peaks (b, c, and d) shifted to low magnetic field ($\Delta\delta$ = 1.29, 1.11, and 0.21 ppm, respectively). Because of reducing electron density of ca. 0.2−0.3 ppm on the oxygen atoms by the coordinated cations, the low-field shifts of these protons (b and c) accompanied with complexation were dominantly due to the reduction of the ring current effects. On the other hand, the oxyethylene proton peak (e) ($\Delta\delta$ = 0.68 ppm) nearest to the benzene ring and aromatic protons (f, g, h, and i) ($\Delta\delta$ = 0.94, 0.28, 0.31, and 1.29 ppm, respectively) shifted to high magnetic field. Especially the aromatic protons (f and i) showed the large high-field shifts ($\Delta\delta$ = ca. 0.94 and 1.29 ppm). This result can be explained by desheilding due to stacking of the benzene and pyrene rings.

On the basis of ^{1}H NMR and fluorescence spectral data, an expected structural change of **4** before and after the addition of metal cation on the ground state is depicted in Figure 4. The oxyethylene moiety and amide group were omitted for clarity.

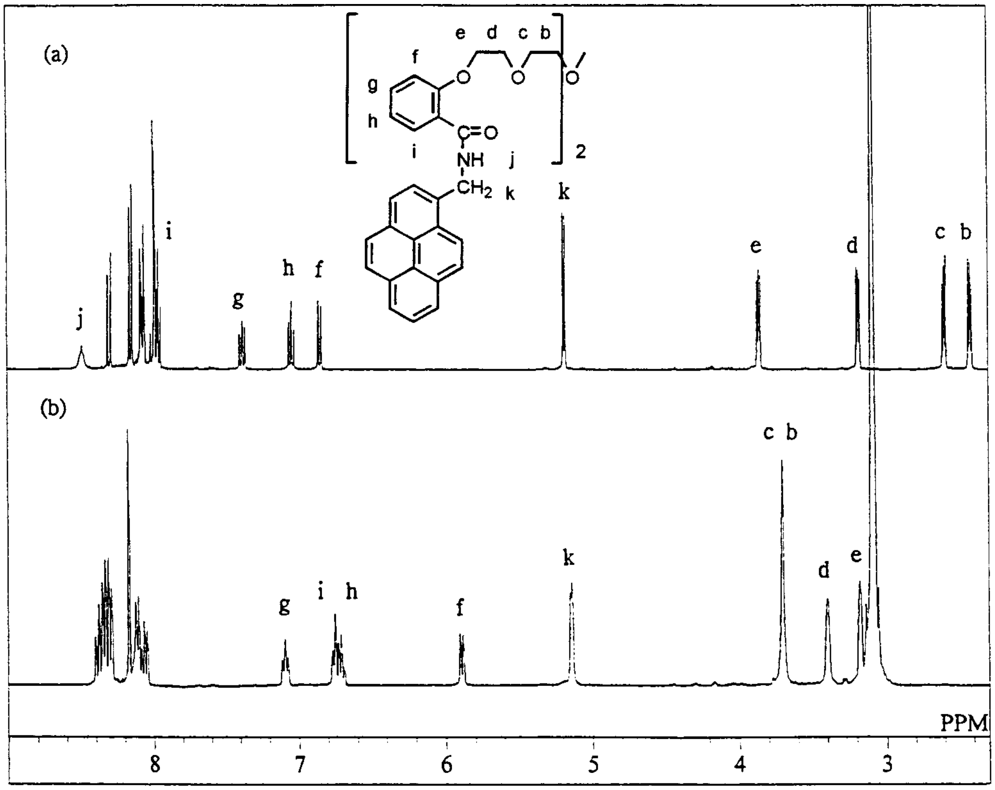

Figure 3. ^{1}H NMR spectra of **4** before (a) and after the addition of Ca^{2+}(b) in acetonitrile-d_3 at 30 °C. [**4**] = 1×10^{-2} mol/dm^3. [$Ca(ClO_4)_2$] = 1 mol/dm^3.

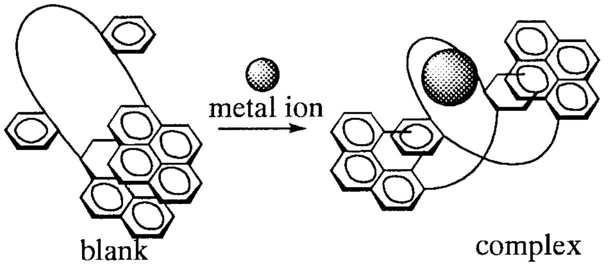

Figure 4. Proposed conformational changes before and after complex formation on the ground state. Amide and oxyethylene moieties are omitted for clarity.

Before the formation of the complex, **4** formed an intramolecular pseudocyclic structure like a crown ether with the aid of a $\pi-\pi$ interaction of two pyrenes, which was supported by the intramolecular excimer emission in the fluorescence spectra. After the addition of metal cations, the complex formed a helical structure, separating two pyrenes. At this time, the pyrene and another side of benzene approached each other and then stacked because of a strong coordination between metal ion and carbonyl group located at the ortho position on benzene. This structural change was also supported by the Corey−Pauling−Koltun (CPK) molecular model study.

Induced chemical shift changes of **3**−**5** on the formation of complexes with various metal ions were listed in Table 2. In the case of **4**·Sr^{2+}, high magnetic field shifts at oxyethylene protons (d) ($\Delta\delta$ = 0.53 ppm) and aromatic protons on the position of (i) ($\Delta\delta$ = 1.4 ppm) and (g) ($\Delta\delta$ = 0.49 ppm) were observed. The aromatic protons (f) to (i) ($\Delta\delta$ = 0.02−1.11 ppm) and oxyethylene proton (e) ($\Delta\delta$ = 0.28 ppm) of **5**·Ba^{2+} indicated high magnetic field shift similar to the chemical shifts in **4**·Ca^{2+}. Although the chemical shift changes of the pyrene protons would give further information, the spectra were too complicated for complete assignments to be made.

Chemical shift changes of **4** in the presence of alkali cations (Li^+, Na^+) were also listed in Table 2. Oxyethylene proton peaks (b, c, and d) shifted to low magnetic field (0.11−0.42 ppm), which strongly indicated that alkali cations were bound to oxyethylene parts. However, oxyethylene proton peak (d) and benzene protons shifted to high magnetic fields, although these amounts (0.17 ppm) were much smaller than those in the case of alkaline earth cations (0.68 ppm). The same trends were observed in the case of **3** and **5**. This shows that the structural changes of the complex **4** with alkali metal ions (Li^+ and Na^+) are smaller than that upon the complexation with alkaline earth cations.

The ^{1}H NMR data of the complex **4**·Mg^{2+} indicate a different behavior from other complexes. The complex **4**·Mg^{2+} had a much smaller value of chemical shift changes (a−i) (0.02−0.6 ppm) than those of **4** with alkaline earth cations (0.21−1.3 ppm for Ca^{2+}), even with strong monomer emission. In addition, the amide proton peak (j) and methylene proton peak (k) shifted to low magnetic field (j, 0.29 ppm; k, 0.07 ppm), although these peaks of other complexes shifted to a high magnetic field. These results suggest that Mg^{2+} does not penetrate so deeply into the oxyethylene moiety but does approach carbonyl oxygen atoms, allowing the reduction of electron density at carbonyl oxygen atoms and then the chemical shift to low magnetic field at amide and methylene proton peaks. The NMR study on the complex of **4** and **3** with Li^+, Na^+, Ca^{2+}, and Mg^{2+} demonstrates that the fluorescence spectral changes originate from the strong coordination of the metal ions on the *o*-carbonyl group and oxyethylene moiety.

The shape of pyrene proton peaks of the complexes in the NMR spectra was quite different from that before addition of the salts (see Figure 3), supporting the occurrence of the conformational changes of two pyrenes. Since it is well-known that the fluorescence lifetime is sensitive to the environment of the fluorescent moieties, we carried out fluorescence lifetime

TABLE 2: Chemical Shifts (δ ppm) of 3−5 and Their Changes at the Complexation with Various Cation Complexes[a]

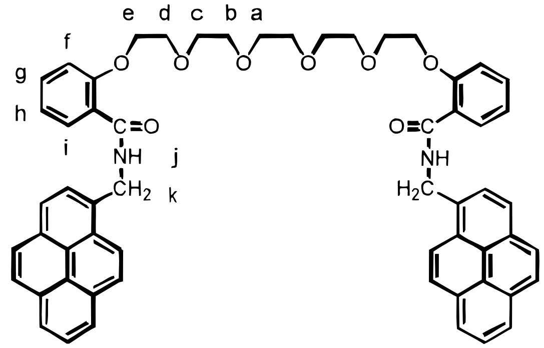

	metal ion	a	b	c	d	e	f	g	h	i	j	k
3	blank			2.00	2.91	3.63	6.72	7.34	7.02	8.01	8.34	5.11
	Li^+			1.26	0.77	0.41	−0.10	−0.15	−0.19	−0.92	−0.62	−0.14
	Ca^{2+}			1.64	1.09	0.68	0.43	0.07	−0.23	−0.78	−0.28	−0.21
	Ba^{2+}			1.62	1.05	0.71	0.42	0.10	−0.07	−0.65	−0.43	−0.06
4	blank		2.42	2.60	3.19	3.86	6.84	7.38	7.05	8.08	8.48	5.18
	Li^+		0.44	0.36	0.06	−0.07	−0.10	−0.02	−0.04	−0.34	−0.14	−0.10
	Na^+		0.42	0.38	0.11	−0.17	−0.27	−0.14	0.16	−0.51	−0.52	−0.10
	Ca^{2+}		1.29	1.11	0.21	−0.68	−0.94	−0.28	−0.31	−1.29	−0.31	−0.03
	Sr^{2+}		*b*	*b*	0.53	−0.27	−0.78	−0.49	−0.37	−1.40	−0.66	−0.17
	Ba^{2+}		1.01	0.99	0.63	0.28	0.02	−0.14	−0.19	−1.11	−0.83	−0.23
5	blank	2.79	2.68	2.79	3.31	3.96	6.92	7.37	7.04	8.11	8.54	5.23
	Li^+	0.12	0.20	0.16	0.0	−0.11	−0.09	0.0	−0.05	−0.37	−0.49	−0.10
	Ca^{2+}	0.29	*b*	*b*	0.19	−0.16	0.09	0.23	−0.31	−1.29	−0.31	−0.03
	Ba^{2+}	*b*	*b*	*b*	−0.16	−0.48	−0.44	−0.05	−0.01	−0.52	−0.27	0.09

[a] Positive values show low field shifts, and negative values show high field shifts. The values in blank show the chemical shifts (δ ppm from TMS) of the protons in acetonitrile-d_3 at 30 °C. [b] These values could not be assigned due to overlapping of peak of water.

TABLE 3: Fluorescence Lifetimes of 3−5 before and after Formation of Complex[a]

	monitored wavelength	
	400 nm (τ/ns)	480 nm (τ/ns)
3	2.5 (74%)	2.5 (−9%)
	120 (26%)	45 (91%)
3·Li^+	4 (3%)	
	60 (97%)	
4	2.1 (18.6%)	2.1 (−4.4%)
	153 (81.4%)	44 (95.5%)
4·Ca^{2+}	142 (100%)	
5	2.7 (8%)	2.2 (−5%)
	127 (92%)	43 (95%)
5·Ca^{2+}	4 (25%)	
	14 (38%)	
	146 (36.5%)	

[a] [**3**]−[**5**] = 1×10^{-6} mol/dm^3, [metal ion] = 1×10^{-3} mol/dm^3, in acetonitrile at room temperature. Negative values in parentheses indicate rising up of excimer from monomer. Excitation = 350 nm.

measurements of pyrene which will bring useful information on the excited-state dynamics of this fluorophore. Table 3 shows the fluorescence lifetimes of **3**−**5** in the presence and absence of metal cations. For the free compounds, decays with two or three exponential components were observed. The results of Table 3 are discussed as follows. The longer lifetimes of >100 ns are due to monomer emissions of pyrene.[42] Fluorescence lifetimes of 10−40 ns correspond to the excimer emissions of pyrene. The short lifetimes from 2 to 4 ns correspond to the transition from monomer to excimer. Complexes that did not give any fluorescence spectral changes had fluorescence lifetimes corresponding to those of a free compound. The lifetimes of both longer-lived and shorter-lived emissions hardly changed upon the complexation, but the magnitudes of the emissions changed. This result shows that the environment around the compounds remained constant upon the complexation.

In the fluorescence spectra, the existence of both excimer and monomer emissions in free and complexed compounds may assume the presence of an intramolecular equilibrium between monomer (M_2*) and excimer (E*) in excited singlet states. As mentioned above, the transformation from monomer to excimer (τ ≈ 4 ns) was much faster than the decay of monomer (τ ≈ 100 ns) or excimer (τ ≈ 40 ns) itself. However, in these cases we should observe only two components in the fluorescence decay. (One corresponds to a transformation from the monomer to excimer in the excited singlet state which gives a decay of monomer emission, and another is a decay of excimer emission.) But three decay components were observed in the present experimental data for free compounds. We have to assume the existence of another excited monomer species. The most plausible one (M_1*) will be the species having a molecular conformation of a rolled-up type where two pyrene moieties fall apart. The probable dynamics of **3**−**5** in the absence of metal ions on the ground and excited states is depicted in Figure 5. From the experimental data, we assign the rate of each step as follows. Compounds **3**−**5** have a slow exchange rate between the rolled-up type (M_1) and the pseudocyclic (M_2) conformations in the ground state. In the excited state, the transition rate between M_1* and M_2* is still slow(τ > 1 μs) whereas the process from M_2* to E* is fast (τ ≈ 4 ns). Under these conditions, the excited monomer M_2* can be converted to the excimer E* in a few nanoseconds. The excited rolled-up monomer M_1* shows the long decay component (ca. 120−170 ns) which is still faster than the conformational change (M_1* → M_2*).

On the other hand, as shown in the fluorescence spectra of the complexes, the metal ions clearly enhanced the formation of the rolled-up type conformation. Thus, the increase in the amount of monomer M_1* species should be observed (Figure 6). In the case of **4**·Ca^{2+}, only one emission around at 400 nm

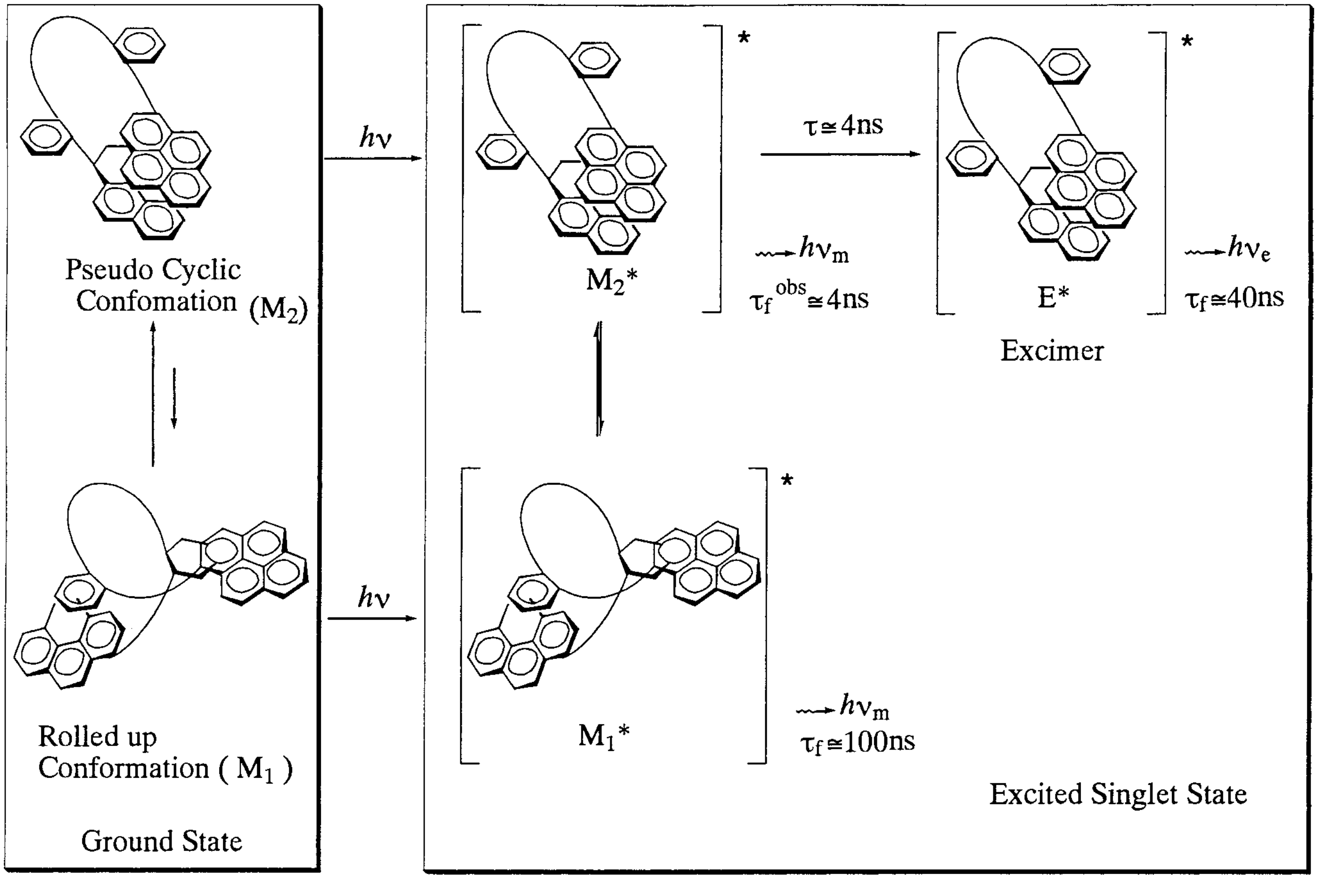

Figure 5. Schematic representation of the kinetics of excited singlet state of **3**−**5** in the absence of metal ions.

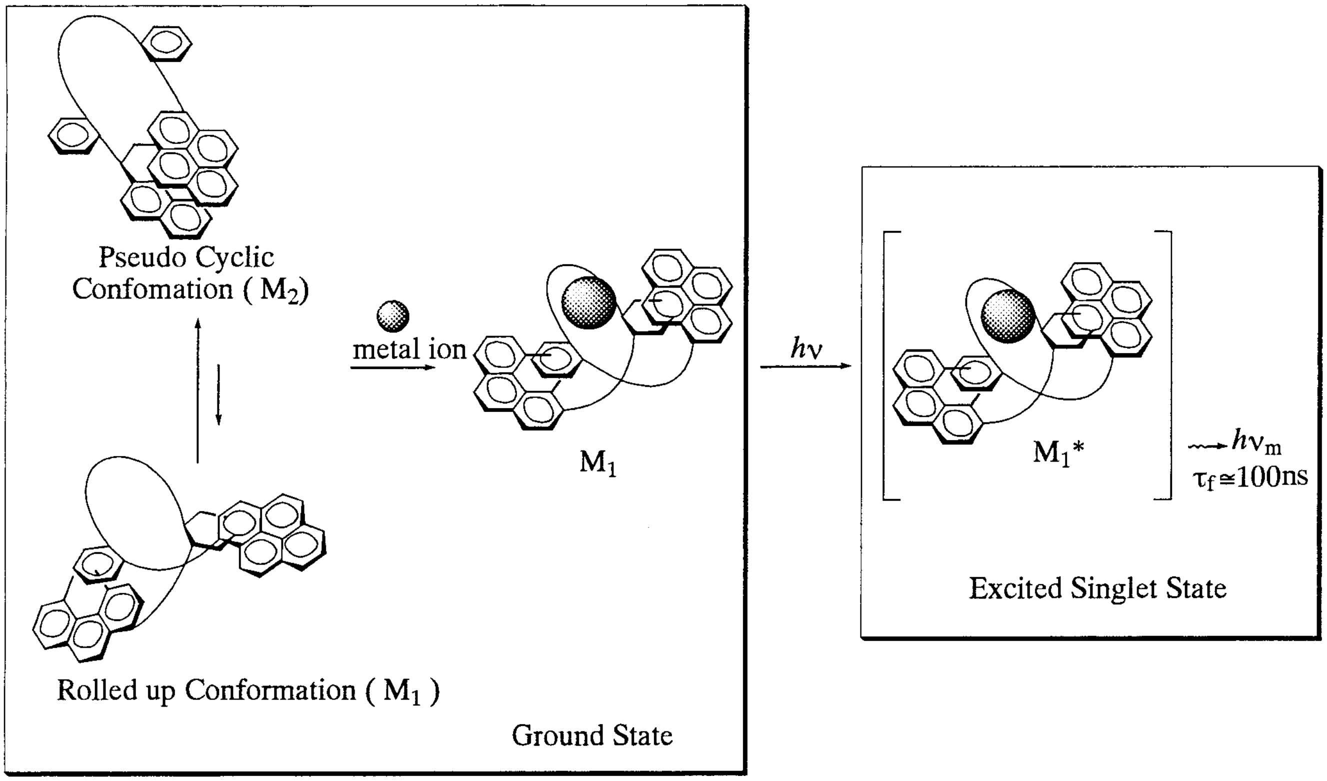

Figure 6. Schematic representation of the kinetics of excited singlet state of **3**−**5** in the presence of metal ions.

was observed, and the transition from monomer to excimer was not detected. This fact indicated that the rolled-up conformation of **4**$\cdot$Ca^{2+} was almost fixed with a strong binding force through the good matching sizes between its cavity and ions. Complex **5**$\cdot$Ca^{2+} showed the enhancement of the monomer emission due to increase of the amount of rolled-up conformation as well as three decay components. This may mean that the conformation of **5**$\cdot$Ca^{2+} is not so rigid compared with that of **4**$\cdot$Ca^{2+} and assume the equilibrium between the rolled-up and the pseudocyclic conformers. The fluorescence lifetimes of **3**·Li^+ indicated the same trend as in the case of **5**·Ca^{2+}. This shows the existence of a slow exchange rate between free and complexed species because the binding constant of **3** for Li^+ is low. As a result, despite the enhancement of the concentration of the rolled-up conformation, three decay components were observed.

Conclusion

The present paper demonstrated the detection of alkali and alkaline earth cations by means of monitoring the fluorescence spectral change of pyrene (intramolecular excimer emission to monomer emission). Stabilization of complex and structural change of the ligand depended on the chain length of oxyethylene moiety and metal cations in the complex, and they could be observed by ^1H NMR and fluorescence spectra. Thus, compound **3** showed the responses specific for Li^+ and Mg^{2+}, which stem from good complementarity between its pseudocavity and the ionic radii of Li^+ and Mg^{2+}. Compounds **4** and **5** responded strongly to alkaline earth cations (Ca^{2+}, Sr^{2+}, and Ba^{2+}).

References and Notes

(1) Down, J. L.; Lewis, J.; Moore, B.; Wilkinsons, G. W. *Proc. Chem. Soc.* **1957,** 209.

(2) Down, J. L.; Lewis, J.; Moore, B.; Wilkinsons, G. W. *J. Chem. Soc.* **1959**, 3767.

(3) Gokel, G. W. *Crown Ethers and Cryptands*; Royal Society of Chemistry: London, 1991.

(4) Choy, E. M.; Evans, D. F.; Cussler, E. L. *J. Am. Chem. Soc*. **1974**, *96*, 7085.

(5) Duax, W. L.; Smith, G. D.; Strong, P. D. *J. Am. Chem. Soc*. **1980**, *102*, 6725.

(6) Vögtle, F.; Weber, E. *Angew. Chem., Int. Ed. Engl*. **1979**, *18*, 753.

(7) Tümmler, B.; Maass, G.; Weber, E.; Wehner, W.; Vögtle, F. *J. Am. Chem. Soc*. **1977**, *99*, 4683.

(8) Yamazaki, N.; Nakahama, S.; Hirao, A.; Negi, S. *Tetrahedron Lett.* **1978**, 2494.

(9) Kubokawa, H.; Yamaguchi, K.; Hirao, A.; Nakahama, S.; Yamazaki, N. *Chem. Lett*. **1982**, 1937.

(10) Yamazaki, N.; Hirao, A.; Nakahama, S. *J. Macromol. Sci., Chem.* **1979**, *A13*, 321.

(11) Kuboniwa, H.; Nagami, S.; Yamaguchi, K.; Hirao, A.; Nakahama, S.; Yamazaki, N. *J. Chem. Soc., Chem. Commun.* **1985**, 1468.

(12) Kuboniwa, H.; Yamaguchi, K.; Hirao, A.; Nakahama, S.; Hori K.; Ohashi, Y. *Chem. Lett*. **1988**, 923.

(13) Kasuga, N.; Nakahama, S.; Yamaguchi, K.; Ohashi, Y.; Hori, K. *Bull. Chem. Soc. Jpn*. **1991**, *64*, 3584.

(14) Gardner, J. O.; Beard, C. C. *J. Med. Chem.* **1978**, *21*, 357.

(15) Hiratani, K.; Aiba, S.; Nakagawa, T. *Chem. Lett.* **1980**, 477.

(16) Hiratani, K. *Chem. Lett*. **1981**, 21.

(17) Hiratani, K.; Sugihara, H.; Kasuga, K.; Fujiwara, K.; Hayashita, T.; Bartsch, R. *J. Chem. Soc., Chem. Commun.* **1994**, 319.

(18) Kakizawa, A.; Akita, T.; Nakamura, H. *Chem. Lett*. **1993**, 1671.

(19) Tahara, R.; Hasebe, K.; Nakamura, H. *Chem. Lett*. **1995**, 753.

(20) Czarnik, A. W. *Fluorescent Chemosensors for Ion and Molecule Recognition*; American Chemical Society: Washington, DC, 1992.

(21) de Silva, A. P.; Gunaratne, H. Q. N.; McCoy, C. P. *J. Am. Chem. Soc.* **1997**, *119*, 7891.

(22) James, T. D.; Sandanayake, K. R. A. S.; Shinkai, S. *Angew. Chem., Int. Ed. Engl.* **1996**, *35*, 1910.

(23) Fabbrizzi, L.; Licchelli, M.; Pallavicini, P.; Perotti, A.; Taglietti, A.; Sacchi, D. *Chem. Eur. J.* **1996**, *2*, 167.

(24) Winkler, J. D.; Bowen, C. M.; Michelet, V. *J. Am. Chem. Soc.* **1998**, *120*, 3237.

(25) Turro, N. J. *Modern Molecular Photochemistry*; University Science Books: Sausalito, 1991; p 141

(26) Hirayama, F. *J. Chem. Phys*. **1965**, *42*, 3163.

(27) Winnik, M. A.; Radpath, T.; Richards, D. H. *Macromolecules* **1980**, *13*, 328.

(28) Cheung, S. T.; Radpath, A. E. C.; Winnik, M. A. *Makromol. Chem.* **1982**, *183*, 1815.

(29) Slomokowski, S.; Winnik, M. A. *Macromolecules* **1986**, *19*, 500.

(30) Radpath, A. E. C.; Svriskaya, P.; Danhelka, J.; Winnik, M. A. *Polymer* **1983**, *24*, 319.

(31) Boileau, S.; Méchin, F.; Martinho, J. M. G.; Winnik, M. A. *Macromolecules* **1986**, *19*, 500.

(32) Eaton, D. F.; Smart, B. E. *J. Am. Chem. Soc.* **1990**, *112*, 2821.

(33) Oyama, H. T.; Hemker, D. J.; Frank C. W. *Macromolecules* **1989**, *22*, 1255.

(34) Aoki, I.; Kawabata, H.; Nakashima, K.; Shinkai, S. *J. Chem. Soc., Chem. Commun.* **1991**, 1771.

(35) Aoki, I.; Sakaki, T.; Shinkai, S. *J. Chem. Soc., Chem. Commun.* **1992**, 730.

(36) Jin, T.; Ichikawa, K.; Koyama, T. *J. Chem. Soc., Chem. Commun.* **1992**, 499.

(37) Takeshita, M.; Shinkai, S. *Chem. Lett*. **1994**, 125.

(38) Inouye, M.; Hashimoto, K.; Isagawa, K. *J. Am. Chem. Soc*. **1994**, *116*, 5517.

(39) Ueno, A.; Suzuki, I.; Osa, T. *J. Am. Chem. Soc*. **1989**, *111*, 6391.

(40) Hayashita. T.; Yamasaki, K.; Konogi, K.; Hiratani, K.; Huang, X.; Jang, D.; McGowen, D. E.; Bartsch, R. A. *Supramol. Chem.* **1996**, *6*, 347.

(41) Marquardt, D. W. *J. Soc. Ind. Appl. Math.* **1963**, *11*, 431.

(42) Pansu, R. B.; Yoshihara, K.; Arai, T.; Tokumaru, K. *J. Chem. Phys.* **1993**, *97*, 1125.